Functional compressive mechanics of a PVA/PVP nucleus pulposus replacement

Abhijeet Joshi[a], Garland Fussell[b], Jonathan Thomas[a], Andrew Hsuan[b], Anthony Lowman[b], Andrew Karduna[c], Ed Vresilovic[d], Michele Marcolongo[a],*

[a]*Department of Materials Science and Engineering, Drexel University, Philadelphia, PA, USA*
[b]*Department of Chemical and Biological Engineering, Drexel University, Philadelphia, PA, USA*
[c]*Department of Human Physiology, University of Oregon, Eugene, OR, USA*
[d]*Department of Biomedical Engineering, Drexel University, Philadelphia, PA, USA*

Abstract

Emerging techniques as an alternative to the current treatments of lower back pain include nucleus replacement by an artificial material, which aims to relieve pain and restore the normal spinal motion. The compressive mechanical behavior of the PVA/PVP hydrogel nucleus implant was assessed in the present study.

PVA/PVP hydrogels were made with various PVP concentrations. The hydrogels were loaded statically under unconfined and confined conditions. Hydrogels were tested dynamically up to 10 million cycles for a compression fatigue. Also, hydrogel nucleus implants with a line-to-line fit, were implanted in the human cadaveric intervertebral discs (IVD) to determine the compressional behavior of the implanted discs.

Hydrogel samples exhibited typical non-linear response under both unconfined and confined compressions. Properties of the confinement ring dictated the observed response. Hydrogel moduli and polymer content were not different pre- and post-fatigues. Slight geometrical changes (mostly recoverable) were observed post-fatigue. In cadavers, hydrogels restored the compressive stiffness of the denucleated disc when compared with equivalent condition of the IVD.

The results of this study demonstrate that PVA/PVP hydrogels may be viable as nucleus pulposus implants. Further studies under complex loading conditions are warranted to better assess its potential as a replacement to the degenerated nucleus pulposus.
© 2005 Elsevier Ltd. All rights reserved.

Keywords: Intervertebral disc; Hydrogel; Mechanical test; Spinal implant; Nucleus pulposus

1. Introduction

Lower back pain is an important socioeconomic disease and one of the most expensive health care issues today. In more than 75% of the cases, the origin of the lower back pain is a degenerated lumbar intervertebral disc (IVD) [1]. In the normal healthy disc, the hydrated nucleus pulposus (nucleus) exerts a hydrostatic pressure (intradiscal pressure (IDP)) on the annulus fibrosus (annulus) fibers [2]. This IDP is mainly responsible for load distribution in the disc, by creating tension in the annulus fibers near the interface with the nucleus. However, this load transfer mechanism is altered in degenerated discs. The water content of the nucleus in the degenerated disc is significantly reduced, resulting in a corresponding decrease in IDP [2–4]. An abnormal stress state of the annulus (which experiences compressive stresses) in the degenerated disc over repeated loading, may provide the stimulus for the formation of cracks and fissures in the annulus and thereby a path for nucleus migration from the center of the annulus toward the periphery.

Total disc arthroplasty [5–7] and nucleus replacement [8,9] are two non-fusion techniques emerging as potential

solutions to this condition. The exploration of these concepts for the alleviation of lower back pain is motivated by the shortcomings of the current treatments, such as spinal fusion and discectomy. Both of these current procedures relieve pain, but do not restore the spinal biomechanics to that of a healthy disc [3,10–13]. Moreover, these procedures may promote further degeneration of either the initially affected disc, in the case of discectomy [12,13] or adjacent IVDs in the case of spinal fusion [14,15]. The ultimate goal of a non-fusion solution for the treatment of lower back pain is to eliminate pain and restore the motion and stress state to that of the normal physiological condition. Nucleus replacement with a synthetic material [8,9,16] or with a tissue engineered structure [17,18] targets earlier stages of disc degeneration (Galante grades I–III) [19], where the annulus is not fully compromised. This approach may help to preserve the annulus and be more amenable to minimally invasive surgical techniques. A classical approach to replacing a diseased or damaged tissue would involve matching the properties of the implant material to those of the normal biological tissue of interest. However, normal nucleus pulposus tissue properties vary with the state of degeneration and has been described with a wide range from a fluid [20] to an isotropic solid [4]. Without a well-defined tissue description, it is difficult to "match" the properties of the tissue.

In order to understand the mechanics of the implant, we need to concurrently understand the mechanics of the implant material. The implant material should be able to withstand mechanical loading states experienced under physiological conditions. While the ideal requirements for a nucleus replacement material have been described [20], test methodologies for determining the device behavior are yet to be agreed on by the regulatory and scientific communities.

Prior work in our laboratory has focused on the development of a chemically stable hydrogel polymer system of polyvinyl alcohol (PVA) and polyvinyl pyrrolidone (PVP) [21–23]. PVA/PVP interactions occur through interchain hydrogen bonding between the carbonyl group of PVP and hydroxyl group of PVA resulting in physical crosslinking of these two polymers. The objective of the current study was to characterize the compressive mechanical properties of a PVA/PVP hydrogel and assess the mechanical feasibility of the material as a potential replacement for the degenerated nucleus of the human lumbar IVD.

2. Materials and methods

2.1. Hydrogel preparation

PVA (Elvanol® Grade 71–30, $M_w = 120,000-140,000$ gm/mol) was obtained from Dupont (Wilmington, DE).

PVP was obtained from Sigma Aldrich (St. Louis, MO) in two different molecular weights ($\overline{M}_n = 10,000$ and $40,000$ g/mol). PVA and PVP powder mixtures were made containing varied PVA/PVP weight ratios between 1% and 5% PVP by weight (where previous data have shown no mechanical differences in modulus in this compositional range [21]) with an equilibrium water content of 84%. The mixtures were dissolved in deionized water at 90 °C for 24 h to yield polymer solutions. The solutions were stirred for 30 min and then cast into cylindrical molds. The molds were then exposed to six consecutive cycles of freezing at -20 °C for 21 h and thawing at 25 °C for 3 h to induce crystallization of the PVA and form physical crosslinking in the hydrogels.

2.2. Unconfined compression tests

Hydrogel samples were made using PVP with $\overline{M}_n = 10,000$ g/mol, as described above. Samples were immersed in phosphate buffered saline (PBS) solution (pH = 7.4) at 37 °C and unconfined compression tests were performed after 1 and 56 days of immersion. The hydrogel samples were loaded in an Instron mechanical testing system (Instron Model 4442, Park Ridge, IL) fitted with a 50-N load cell. Samples were compressed at a strain rate of 100% strain/min. Load and displacement data were recorded at 20 Hz with the Instron Series IX software. These data were converted to stress–strain values and a tangent compressive modulus for each hydrogel sample was calculated at 15%, 20%, and 25% strain. The average slopes of a linear trend line formed with the stress–strain data from 10–20%, 15–25%, 20–30% were assumed equal to the tangent slopes at 15%, 20%, and 25% strain, respectively.

2.3. Unconfined compressive fatigue behavior

2.3.1. Fatigue tests

Samples ($n = 9$) were made with PVP having $\overline{M}_n = 40,000$ g/mol, according to the methods described above. The hydrogel samples were axially compressed to 15% strain for 100,000, 1, and 10 million cycles at 5 Hz in PBS solution (pH = 7.4) at 37 °C with an Instron Model 1331. The tests were run with a preload of approximately 9 N. Three samples were tested under each condition. Surfaces with circular grooves were used on the testing apparatus to keep the test samples stationary during testing. The 15% strain represents the approximate strain corresponding to load on the intact IVD under physiological conditions [2,24]. The mass and dimensions of the samples were measured before and after fatigue cycling. Samples were placed back in PBS solution at 37 °C for 14 days, with mass and dimensions measured daily.

Unconfined compression tests were performed on each sample before and after fatigue test. The compressive modulus was calculated to determine the effect of fatigue cycling on the stiffness of the hydrogels. The samples were compressed at a strain rate of 100% strain/min. The tangent compressive modulus was calculated at 15%, 20%, and 25% strain as described earlier.

2.3.2. Mass, dimension, and density measurements

Mass of the hydrogels was measured with a Denver Instruments M-120 balance. After fatigue, samples were weighed in both air and heptane, and then dried under vacuum. The dry mass of the samples in air was then measured and recorded. To calculate the dry mass percentage for the hydrogels, the dry mass after fatigue was divided by the wet mass after fatigue. Measurements of the height and diameter were taken for each sample before and after fatigue testing, and for 14 days after fatigue, using a digital caliper. The density of the hydrogels was calculated by taking the mass in heptane and using Eq. (1), where $\rho_{hydrogel}$ is the density of the hydrogel, $\rho_{heptane}$ is the density of heptane, m_{air} is the mass of the hydrogel in air, and $m_{heptane}$ is the mass of the hydrogel in heptane:

$$\rho_{hydrogel} = \frac{\rho_{hydrogel} \times m_{air}}{(m_{air} - m_{heptane})}. \tag{1}$$

2.4. Confined compression testing

Hydrogels were made with PVP having $\overline{M}_n = 10,000 \, g/mol$, as described previously [21,22]. A confined compressive modulus was calculated by using a confined compression testing configuration fitted to an Instron mechanical testing system (Model 4442, Park Ridge, IL). Samples were compressed at a strain rate of 100% strain/min. A cylindrical plunger was compressed upon the gel as it was confined by a ring of either silicon rubber ($n = 5$) or high-density polyethylene (PE) ($n = 5$). The silicon rubber ring has a modulus (approximately 1.0 MPa) closer to that of the PVA/PVP hydrogel allowing radial deformation of the ring upon loading of the hydrogel. The high-density PE ring was considered a rigid body, as its modulus (approximately 1.0 GPa) is several magnitudes higher than that of the hydrogel sample it surrounded. Load and displacement data were recorded at 20 Hz with Instron Series IX software. These data were converted to stress–strain values and confined compressive modulus was calculated as described earlier.

2.5. Human cadaver mechanical testing

2.5.1. Specimen preparation

Hydrogels were prepared with PVP having $\overline{M}_n = 10,000 \, g/mol$, as described earlier. Anterior column units (ACUs) were harvested from 8 cadavers (3 males and 5 females) with an average age of 65 years, within 72 h of death. An ACU is defined as an IVD with the superior and inferior vertebra, but with the muscle and posterior elements removed from the vertebral bodies. Fifteen lumbar ACUs from L1-S1 levels were selected based on visual inspection, eliminating those with obvious damage or degeneration. Parallel cuts were made perpendicular to the longitudinal axis of the ACU, through the vertebrae superior and inferior the disc to ensure alignment of the axial compression load. Anatomical measurements of the specimen (disc height, superior and inferior vertebrae height, disc major and minor diameters) were performed using standard digital calipers.

2.5.2. Mechanical testing procedure

The test specimen was constrained in a custom-made test fixture with help of screws, which connected the inferior vertebrae to the test fixture. A commercially available potting mixture (Cargroom; US Chemical and Plastics, OH, USA) was used for potting of specimens in the fixture. Only the inferior vertebra was potted. The superior vertebra was compressed against a flat compression plate attached to the load cell. Specimens were kept moist throughout the experiment by spraying with a protease inhibitor.

2.5.3. Compression testing protocol

An Instron (Model 1331; Canton, MA, USA) mechanical testing machine was used. The initial baseline position of the upper compression plate and lower actuator was ensured and maintained through each test condition. The specimens were preconditioned for 50 cycles at 3% strain (based on the average IVD height). Specimens were axially compressed to 15% of total average IVD height. The testing was performed with a triangular waveform at 0.5 Hz with a loading rate of 15% strain/s for 5 loading cycles, for each tested condition.

2.5.4. IVD implantation and test protocol

A series of axial compressive tests were completed on each specimen, as shown in Fig. 1. First, the intact specimen was tested using the compression testing protocol (intact condition). Then, a Cloward core drill bit of 16 mm diameter was used to drill perpendicular to the cut surface of the superior vertebra through the bone to the IVD. A cylindrical bone plug above the disc was removed. For the second test condition, (BI condition), the cylindrical bone plug was reinserted and the test protocol was repeated. Then, the bone plug was removed from the ACU and the central portion of the nucleus in line with the core drill (equal to 16 mm diameter) was removed using standard surgical instruments, keeping the residual nucleus and the annulus intact (Fig. 2). The testing protocol was then run on the denucleated specimen without the bone plug (DN-1, denucleated condition). A cylindrical hydrogel implant with a diameter equal to 16 mm and height equal to that of measured average disc height was implanted into the cavity formed by removal of the nucleus material. This formed a line-to-line fit of the nuclear defect. The bone plug was again placed in its original position over the hydrogel implant and the testing protocol was repeated (implanted condition). Finally, the implanted hydrogel and bone plug were removed and the specimen was tested again (DN-2, denucleated
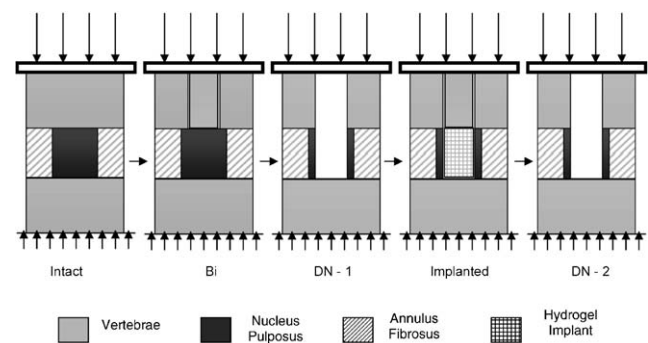

Fig. 1. Schematic of test procedure and implantation method of a lumbar anterior column unit.
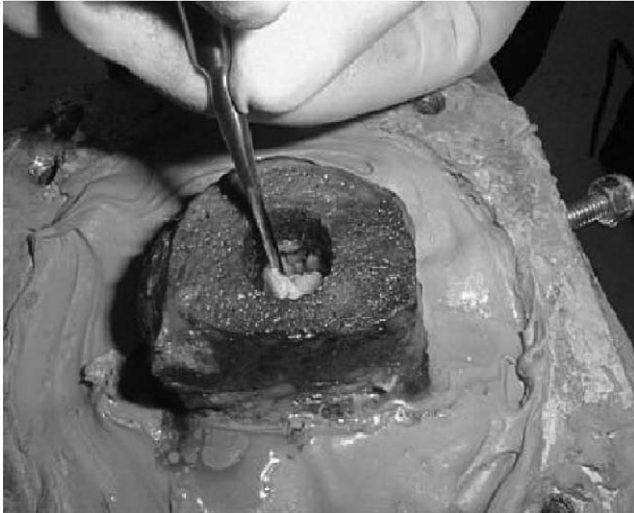
Fig. 2. Denucleated anterior column unit test specimen.

condition) to determine if there was any damage to the specimen during testing.

2.5.5. Data analysis

The load–displacement history data for each test condition were collected using a Labview® program (sampling rate = 1000 Hz). Data for the fifth loading cycle were taken for analysis and instantaneous compressive stiffness values (N/mm) were calculated at representative strain levels of 5%, 10% and 15%, for each condition, for each specimen. The stiffness values were obtained by numerically differentiating the raw data, taking the slope of the line passing through points corresponding to the representative strain levels. For each strain level (5%, 10% and 15%), a one-way, repeated measures ANOVA was performed for compressive stiffness with one subject factor (surgical condition: intact, BI, DN-1, implanted, DN-2). Follow up paired *t*-tests were conducted to assess the effect of surgery (intact vs. BI), effect of denucleation (BI vs. DN-1), restoration ability of the hydrogel (BI vs. implanted) and crosscheck (DN-1 and DN-2). The acceptable rate for a type-I error was chosen as 5% for all tests.

3. Results

3.1. Unconfined compression tests

Under unconfined compression, PVA/PVP hydrogels typically show a non-linear stress–strain response (Fig. 3a). The tangent modulus values at 15%, 20% and 25% strain were 0.23, 0.29 and 0.37 MPa, respectively (Fig. 3b). The effect of PVP content on the mechanical stiffness of the gels was studied. Side-by-side compression tests of gels processed for this study with different PVA/PVP weight ratios were performed after 1 and 56 days of immersion in PBS at 37 °C. Hydrogels with the different ratios of PVA to PVP had the same mechanical properties, even after 56 days of immersion in PBS.
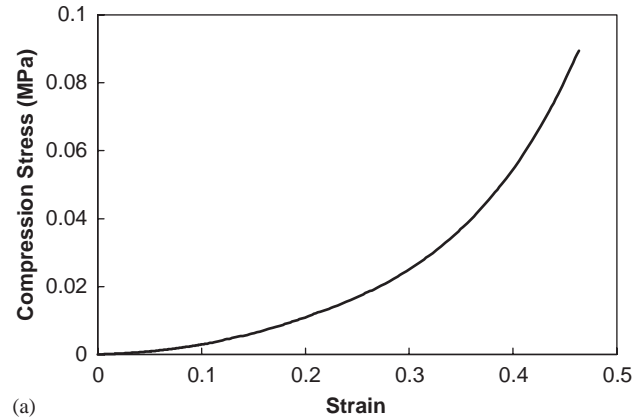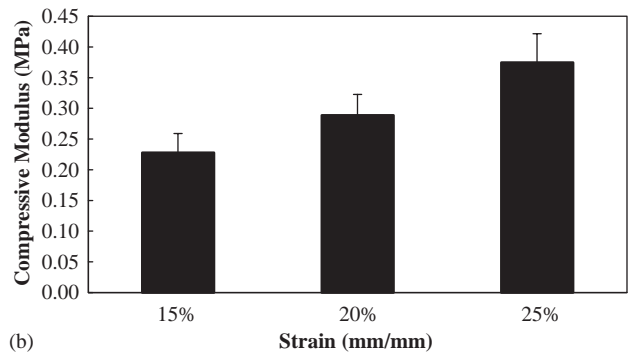
Fig. 3. (a) Typical unconfined compression stress–strain curve showing hyperelastic response. (b) The unconfined compression modulus increases as the strain magnitude increases.

3.2. Unconfined compressive fatigue behavior

The normalized compressive modulus was determined for the hydrogels at 15, 20 and 25% strain after fatigue testing (Fig. 4). The moduli of the fatigued samples were normalized to the un-fatigued control hydrogels. The moduli of the hydrogel samples subjected to no fatigue, 100,000, and 1 million cycles were all within standard deviations (at 15%, 20% and 25% strain). There was a 24% decrease in the modulus at 15% strain, for the samples after 10 million cycles. However, the modulus for these samples at 20% and 25% strain was not different from the controls.

Fig. 5a shows the normalized diameter and height of the hydrogel that had been subjected to 100,000 fatigue cycles. All the hydrogels showed some changes in the geometry post-fatigue, which were recovered (compared to the controls) within one day of unrestrained recovery in PBS. The normalized diameter and height after 14 days in PBS is presented in Fig. 5b. A 5% increase in diameter and a 17% decrease in height were observed after 10 million cycles. The polymer content (indicated by dry mass) of the hydrogels (Fig. 6) and the post-fatigue density (compared with original density of 1.04 g/cm^3) showed no appreciable change with any number of fatigue cycles. This is consistent with
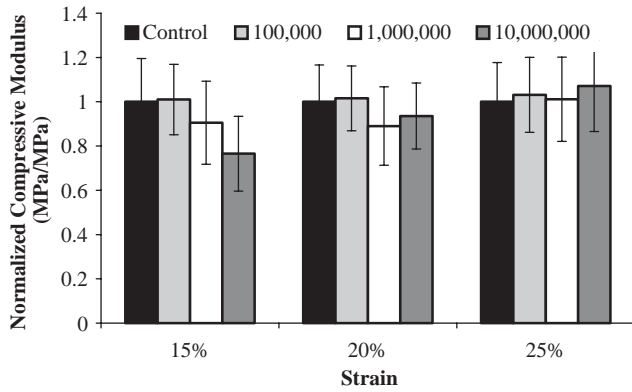
Fig. 4. Compressive modulus at 15%, 20% and 25% strain before and after fatigue of up to 10 million cycles. There was a small reduction in modulus at 15% strain after 10 million cycles; however, there were no significant differences in moduli up to 10 million cycles for 20% and 25% strain levels ($p > 0.05$).
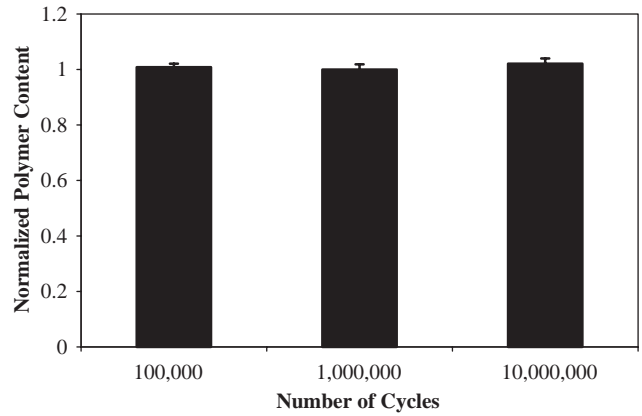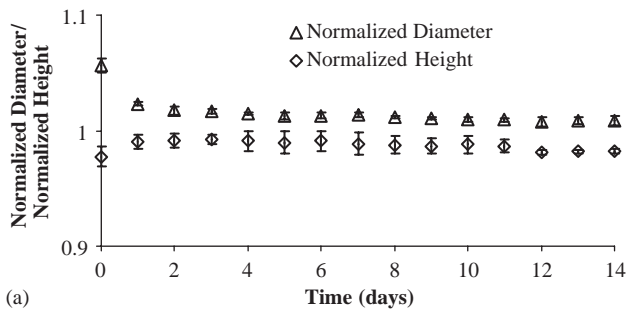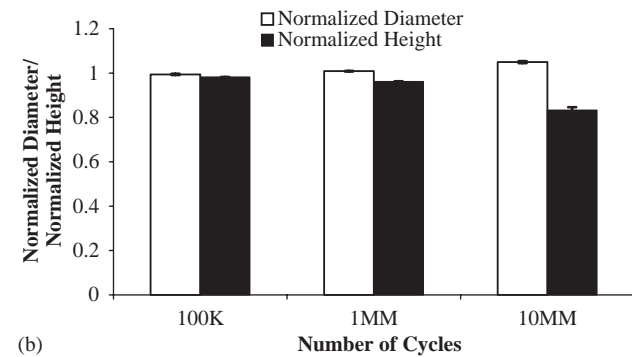

Fig. 6. There was no significant change in the normalized polymer content of the samples after fatigue through 10 million cycles ($p > 0.05$).

(a)

(b)

Fig. 5. (a) Normalized diameter and height recovery for the PVA/PVP hydrogel after 100,000 fatigue cycles. Diameter increased from control dimensions by 5% upon removal from test fixture, however, after 2 days recovery, the samples returned to original dimensions. Height showed a slight decrease after fatigue, but recovered within two days. (b) Normalized diameter and height 14 days after removal from fatigue setup. No statistically significant differences were measured after 10 million cycles after 14 days of recovery for diameter. Up to 1 million cycles, there were no significant differences in height from before testing. However, the 10 million cycle samples showed a height reduction of approximately 17% ($p < 0.05$).
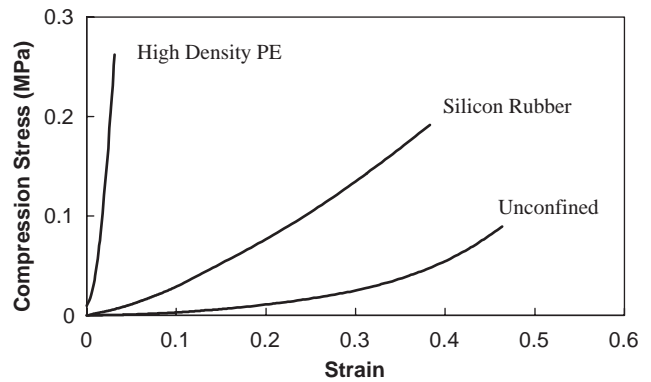

Fig. 7. Comparison of typical stress–strain responses of PVA/PVP hydrogels obtained using two different confinement rings: silicon rubber, high-density PE. A typical stress–strain response of a PVA/ PVP hydrogel in the unconfined condition is also provided for reference.

3.3. Confined compression tests

Typical stress–strain responses of two confined compression tests (using silicon rubber and high-density PE as confinement rings) are compared with a typical unconfined stress–strain response for a PVA/PVP hydrogel (Fig. 7). The high-density PE ring is stiffer than the silicon rubber ring and thus results in a stress–strain curve with a higher slope. The average confined moduli were 0.19 MPa with silicone rubber ring and 12.70 MPa with high-density PE ring.

3.4. Human cadaver mechanical testing

The non-linear load–displacement behavior was observed for all specimens under all conditions (Fig. 8a). Fig. 8b shows the plot of ACU compressive instantaneous stiffness (N/mm) vs. the strain (%) for all five testing conditions. The one-way ANOVA calculations comparing stiffness of these five conditions at 5%, 10%

previous work showing mass stability of PVA/PVP physically cross-linked systems in an unloaded environment in vitro [21].
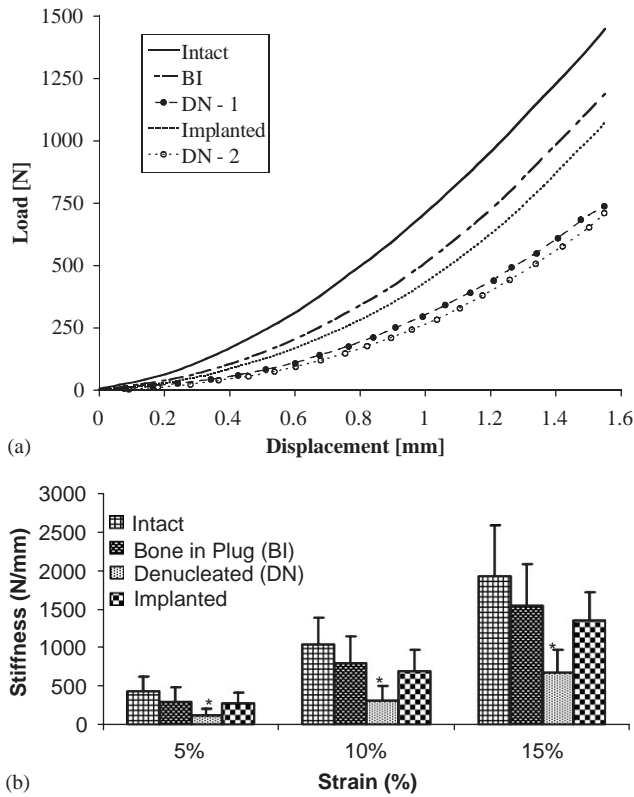
Fig. 8. (a) Load–displacement behavior of one test specimen for different test conditions. (b) Compressive stiffness (N/mm) vs. compressive strain (%) for different test conditions.

Table 1
Compressive stiffness comparison of denucleated specimen, hydrogel implant alone and implanted specimen

Stiffness (N/mm)	5% Strain	10% Strain	15% Strain
Denucleated	116.0	311.0	672.0
Hydrogel implant	0.8	1.7	2.5
Implanted	277.0	702.0	1351.0

4. Discussion

Nucleus replacement is emerging as a possible minimally invasive treatment for the pervasive condition of degenerative disc disease. Our approach to this challenging engineering problem is to utilize highly compliant, elastomeric hydrogels as nucleus replacement materials. Upon loading, the device is designed to create a stress on the internal surface of the annulus that will mimic the IDP of the normal nucleus pulposus. In this work, we were interested in characterizing the compressive mechanical behavior of PVA/PVP hydrogels and determining the functional compressive behavior of a nucleus-implanted IVD.

Until recently, hydrogels have not been considered as load-bearing devices due to the limited mechanical properties. Some work has begun to examine hydrogels for use in nucleus [21,25–28] and cartilage replacements [29–31]. Stammen et al. [29] have shown the compressive behavior of PVA hydrogels for different polymer contents and strain rates. For hydrogels of 20% polymer content (at 100% strain/min), they reported unconfined compressive tangent moduli in the range of 1.5–2.0 MPa for PVA cryogels at 20% strain. This can be compared to our results where 10% PVA/PVP hydrogels exhibited a compressive tangent modulus of 0.29 MPa at 20% strain. Differences in the modulus values may be attributed to the differences in polymer content and processing conditions. Although the overall polymer content affects the compressive modulus, varying the PVA/PVP ratios did not significantly affect the modulus, even after 56 days of immersion in PBS. There was, however, an increase in modulus with immersion for each group, which is attributed to the equilibration of the hydrogel material system with water, which has been shown to occur after about 14 days [32].

The compressive moduli of the samples at 15% strain were unchanged after 1 million cycles of unconfined compressive fatigue. The initial portion of the compression curve was flatter for the 10 million cycle samples, producing a lower modulus at 15%. The curve recovered the shape of the other samples at higher strains, resulting in no change in modulus, showing that the samples were still intact and structurally unchanged.

There was no change in diameter of samples (for 100,000 and 1 million cycles), and no change in height of

and 15% strain showed significant differences ($p < 0.001$). In all the specimens (at 5%, 10%, 15% strain), the stiffness for the denucleated conditions (DN-1 vs. DN-2) was not significantly different ($p = 0.92$, 0.60, and 0.23, respectively), indicating a return to the original denucleated condition after implant removal.

Drilling into the vertebrae (BI) reduced the stiffness compared to the intact condition and was significantly different (e.g. stiffness value 80% of intact at 15% strain, $p < 0.001$ at all strains levels). A more dramatic reduction in the stiffness was observed for denucleated specimens (e.g. stiffness value 44% of BI at 15% strain, $p < 0.001$ at all strain levels). Insertion of the hydrogel implant restored the stiffness of the ACU to a value of 88% of BI at 15% strain and was significantly different than DN-1 at all strain levels ($p < 0.001$). This restoration of stiffness by the hydrogel implant was 92%, 88% and 88%, of BI stiffness at respective strain levels. Stiffness of BI compared to implanted was not significantly different ($p > 0.05$) at all strain levels.

The effect of hydrogel implantation in the denucleated specimen is clearly shown in the resulting increased stiffness of the implanted specimen (Table 1). Moreover, the implanted specimen stiffness is far greater than the corresponding algebraic sum of the denucleated specimen stiffness and the hydrogel.

samples (for 100,000 cycles). This indicates that the initial deformations were reversible during the 14 days of immersion following the fatigue tests. The increase in the diameter of the hydrogels (for 10 million cycles) and the decrease in height of the hydrogels (for 1 and 10 million cycles) are permanent, and may have been a result of creep. Creep is usually associated with samples that have been subjected to a static load [33]. However, with 10 million cycles at 5 Hz, the cumulative fatigue could have produced a creep effect in the samples due to polymeric chain relaxation, resulting in the dimension change. The samples which recovered their approximate original dimensions were subjected to reversible creep, possibly because of a temporary change in water content during the fatigue testing. Additionally, there was no change in the dry mass percent of the samples after 14 days of recovery, independent of number of fatigue cycles. The fact that the density of the samples did not change after 10 million fatigue cycles is another confirmation that the composition of the hydrogels remained unchanged.

In functional use as a nucleus pulposus replacement, the implant would be in contact with the surrounding annulus fibrosus, ideally in a line-to-line or press fit condition [24,34]. A cylindrical hydrogel that is being compressed axially will expand radially because of its high Poisson's ratio. A hydrogel axially compressed within a silicone confinement ring having a relatively similar stiffness will transfer loads to the ring, causing the ring to expand radially. The expansion of this relatively compliant ring results in a much lower confined compression modulus compared to that resulting from a rigid ring, such as high density PE. There is a two order of magnitude difference in compressive modulus between the unconfined and silicone confined conditions.

The confined compression test is similar to our in vitro human cadaveric tests where a hydrogel implant (having line-to-line fit) was replaced in the artificially created nucleus cavity of the lumbar IVD with an intact surrounding annulus. Earlier work has been performed for nucleus replacement with a synthetic material in cadaveric ACUs [35] and in animals [36]. Meakin et al. [36] used sheep discs to assess the effect of nucleus implant on bulging direction of the annulus fibers, in pure compression. However, in all of the cases, the nucleotomy was facilitated by making a small incision through annulus. Our novel approach to nucleus implantation precluded annulus damage [24,34], enabling full interaction of the nucleus implant and intact annulus.

Calculated stiffness values for intact specimens agreed well with those previously reported for lumbar ACUs in the literature (772–3040 N/mm) [2,37]. The restoration of stiffness to the denucleated ACU after implantation with the PVA/PVP hydrogel is evident from Fig. 8. The general premise that the IVD biomechanics and load transfer mechanism results from synergistic effect between the implanted hydrogel and the surrounding intact annulus is shown through this study. Considering the data in Table 1, one can clearly see that the summation of the stiffness of the 'denucleated' ACU (e.g. 672 N/mm at 15% strain) and that of 'hydrogel only' (e.g. 2 N/mm at 15% strain) is far less than the stiffness of the 'implanted' ACU (e.g. 1351 N/mm at 15% strain). This non-linear increase in the stiffness observed after implantation of the polymeric hydrogel is due to the interaction between the polymeric implant and the intact annulus. Poisson's ratio of the hydrogel results in a significant radial displacement in compression. In an intact disc, load transfer occurs by pushing the annulus radially outwards, which is facilitated by IDP, generated by the hydrated nucleus pulposus. In the denucleated disc, the inner annulus fibers bulge inwards and are in compression. In the nucleus-implanted disc, the radial displacement of the implant causes a stress at the implant/annulus interface (Fig. 9). This stress mimics the IDP of a normal nucleus and presumably creates tension in annulus fibers. The tension in the annulus fibers then allows the annulus to bear more loads, resulting in higher stiffness of the ACU, through this synergistic interaction [24].

Only compressive mechanics of the PVA/PVP hydrogel implant was examined in this work. Although, compression is the major load acting on the IVD, other loading modes or, combination of loading modes such as flexion-extension, torsion and lateral bending generally leads to worst case loading scenario, from IVD point of view. The results presented here may not necessarily hold true for other loading modes and should also be viewed in terms of the limited sample size and age of the cadaveric specimens tested. The in vitro method used for implantation purposes is certainly not viable clinically. The work done was only to assess the compressive hydrogel nucleus implant mechanics, without damage to the annulus and further work is needed to better understand the static and dynamic behavior of the PVA/PVP hydrogel nucleus implant under complex physiological loading conditions.

5. Conclusion

The compressive mechanical behavior of the PVA/PVP hydrogel implant, which would serve as a potential replacement to the degenerated nucleus of the IVD, was detailed. The unconfined compression testing and the confined compression testing of the hydrogel implant (simulating the in situ annulus structure) showed a non-linear stress–strain behavior, typical of soft tissue. Higher modulus was observed for samples subjected to confined compression than for the samples tested in an
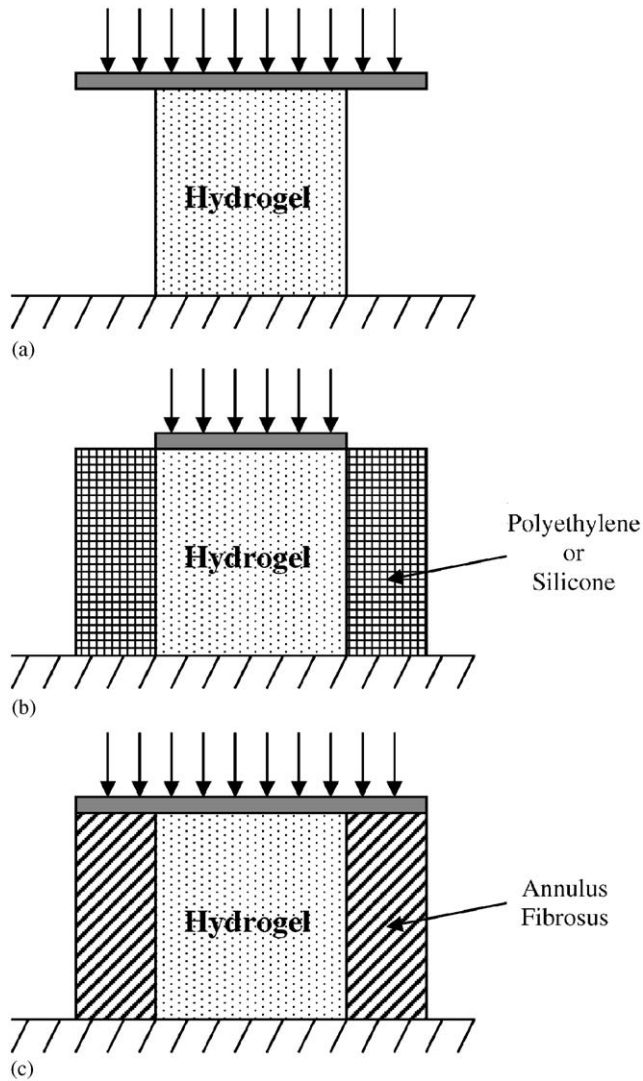
Fig. 9. (a) Unconfined compression test of a hydrogel implant. (b) Confined compression test of a hydrogel implant in a construct of comparatively rigid material simulating bulk modulus effect. (c) Cadaveric mechanical testing of a hydrogel implanted intervertebral disc with comparatively rigid annulus fibrosus simulating confined compression test.

unconfined condition and the properties of the con-straining ring directly affected the observed properties of the confined specimens. No appreciable alteration in mechanical behavior of the hydrogels after 10 million cycles of compression–compression fatigue to 15% displacement was observed. This was accompanied by mass stability and slight geometrical changes which were mostly recoverable. The in situ studies were further supported by in vitro studies where the PVA/PVP hydrogel implant replaced the nucleus of the human lumbar IVD. The implanted hydrogels were able to restore the compressive stiffness properties of the equivalent ACU. A synergistic effect between the implant and the surrounding tissue was observed.

Nucleus replacement by a PVA/PVP hydrogel may provide an enhanced long-term outcome as compared to the current treatment methods of lower back pain like discectomy and fusion.

References

[1] MedPro Month VIII, 1998.
[2] White AA, Panjabi MM. Clinical biomechanics of the spine, II ed. Philadelphia: J.B. Lippincott Company; 1990.
[3] Bao QB, McCullen GM, Higham PA, Dubleton JH, Yuan HA. The artificial disc: theory, design and materials. Biomaterials 1996;17(12):1157–66.
[4] Iatridis JC, Weidenbaum M, Setton LA, Mow VC. Is the nucleus pulposus a solid or a fluid? Mechanical behaviors of the nucleus pulposus of the human intervertebral disc. Spine 1996;21(10):1174–84.
[5] Salib RM, Pettine KA. Intervertebral disk arthroplasty. US Patent No. 5258031, 1993.
[6] Patil A. Artificial intervertebral disc. US Patent No. 4309777, 1982.
[7] Baumgartner W. Intervertebral disk prosthesis. US Patent No. 5320644, 1994.
[8] Nachemson AL. Some mechanical properties of the lumbar intervertebral disc. Bull Hosp Jt Dis (NY) 1962;23:130–2.
[9] Fassie B, Ginestle JF. Disc prosthesis made of silicone—experimental study and first clinical cases. Nouvelle Presse Med 1978;21:207.
[10] Weber H. Lumbar disc herniation: a controlled prospective study with ten years of observation. Spine 1993;8:131–40.
[11] Kambin P, Savitz MH. Arthroscopic microdiscectomy: an alternative to open disc surgery. Mt Sinai J Med 2000;67(4):283–7.
[12] Goel VK, Goyal S, Clark C, Nishiyama K, Nye T. Kinematics of the whole lumbar spine—effect of discectomy. Spine 1985;10:543–54.
[13] Tiberwal SB, Pearcy MJ, Portek I, Spivey J. A prospective study of lumbar spinal movements before and after discectomy. Spine 1985;10:455–9.
[14] Lee CK, Langrana NA. Lumbosacral spinal fusion: a biomecha-nical study. Spine 1984;9:574–81.
[15] Leong JC, Chun SY, Grange WJ, Fang D. Long term results of lumbar intervertebral disc prolapse. Spine 1983:793–9.
[16] Chan M, Chowchuen P, Workman T, Eilenberg S, Schweitzer M, Resnick D. Silicone synovitis: MR imaging in five patients. Skeletal Radiol 1998;27(1):13–7.
[17] Gan JC, Ducheyne P, Vresilovic E, Shapiro I. Bioactive glass serves as a substrate for maintenance of phenotype of nucleus pulposus cells of the intervertebral disc. J Biomed Mater Res 2000;51(4):596–604.
[18] Shirazi A, Shrivastava SC, Ahmed SM. Stress analysis of the lumbar disc-body unit in compression. Spine 1984;9(2):120–34.
[19] Galante JO. Tensile properties of the human annulus fibrosus. Acta Orthop Scand 1967;100(Suppl.):4–91.
[20] Bao QB, Yuan HA. Prosthetic disc replacement: the future? Clin Orthop Rel Res 2002;394:139–45.

[21] Thomas J, Lowman A, Marcolongo M. Novel associated hydrogels for nucleus pulposus replacement. J Biomed Mater Res 2003;67A:1329–37.

[22] Thomas J, Gomes K, Lowman A, Marcolongo M. The effect of dehydration history on PVA/PVP hydrogels for nucleus pulposus replacement. J Biomed Mater Res Pt B: Appl Biomater 2004; 69(2):135–40.

[23] Liu X, Marcolongo M, Lowman A. Short term in vitro response of associating hydrogels. Macromolecules, in press.

[24] Joshi A. Mechanical behavior of the human lumbar intervertebral disc with polymeric hydrogel nucleus implant: an experimental and finite element study. PhD. thesis, Drexel University, Philadelphia PA; 2004.

[25] Bagga CS, Wiliams P, Higham PA, Bao QB. Development of fatigue test model for a spinal nucleus prosthesis with preliminary results for a hydrogel spinal prosthetic nucleus. In: Bioengineering conference BED, vol. 1997; 1997. p. 441–2.

[26] Ray CD. In: Weinstein JN, editor. Clinical efficacy and outcome in the diagnosis and treatment of low back pain. New York: Raven Press, Ltd.; 1992. p. 205–25.

[27] Bao QB, Higham PA. Hydrogel intervertebral disc nucleus. US Patent No. 5047055, 1991.

[28] Bao QB, Higham PA. Hydrogel intervertebral disc nucleus. US Patent No. 5192326, 1993.

[29] Stammen JA, William S, Ku DN, Guldberg RE. Mechanical properties of a novel PVA/PVP hydrogel in shear and unconfined compression. Biomaterials 2001;22:799–806.

[30] Bryant SJ, Anseth KS. Controlling the spatial distribution of ECM components in degradable PEG hydrogels for tissue engineering cartilage. J Biomed Mater Res 2003;64A: 70–9.

[31] Hutmacher DW, Ng KW, Kaps C, Sittinger M, Klaring S. Elastic cartilage engineering using novel scaffold architectures in combination with a biomimetic cell carrier. Biomaterials 2003;24:4445–58.

[32] Fussell G, Thomas J, Scanlon J, Lowman A, Marcolongo M. The effect of protein-free versus protein-containing medium on the mechanical properties and uptake of ions of PVA/PVP hydrogels. J Biomater Sci Polym Ed 2005;16(4):489–503.

[33] Li JCM. Impression creep and other localized tests. Mater Sci Eng 2002;A322:23–42.

[34] Joshi A, Vresilovic E, Marcolongo M, Lowman A, Karduna A. Proceedings of the 29th annual meeting. Society for Biomaterials 2003:214.

[35] Eysel P, Rompe JD, Schoemayr R, Zoellner J. Biomechanical behvaior of a prosthetic lumbar nucleus. Acta Neurochir (Wien) 1999;141:1083–7.

[36] Meakin JR, Reid JE, Hukins DWL. Replacing the nucleus pulposus of the intervertebral disc. Clin Biomechan 2001;16:560–5.

[37] Langrana NA, Edwards WT, Sharma M. Biomechanical analyses of loads on the lumbar spine. In: Wiesel SW, Weinstein J, Herkowitz H, Dvorak J, Bell G, editors. The lumbar spine. Philadelphia: W.B. Saunders Company; 1996. p. 163–71.